DESIGN CONCEPTS OF A BEAM SPREADER FOR A NEXT GENERATION FREE ELECTRON LASER*

M. Placidi#, P. J. Emma, J.-Y. Jung, G. C. Pappas, D. S. Robin, C. Sun, W. Wan
Lawrence Berkeley National Laboratory, Berkeley, CA 94720, USA

Abstract

Lawrence Berkeley National Laboratory (LBNL) is developing design concepts for a multi-beamline soft x-ray FEL array powered by a superconducting linear accelerator, operating with a high bunch repetition rate of approximately one MHz. Electron bunches supplied by a high-brightness, high-repetition-rate photocathode electron gun are distributed by a beam spreader, designed to deliver individual bunches from a CW linac to an array of independently configurable FEL beamlines with nominal bunch rates up to 100 kHz in each FEL, and with even pulse spacing. We describe recent developments in the technical choices, design and parameters of the spreader system and its main components.

ELECTRON BEAM SPREADER REQUIREMENTS

Lawrence Berkeley National Laboratory (LBNL) is developing design concepts for a multi-beamline soft x-ray FEL array powered by a superconducting linear accelerator, operating with a high bunch repetition rate of approximately one MHz [1]. Electron bunches supplied by a high-brightness, high-repetition-rate photocathode electron gun and accelerated to a maximum energy of ~2.6 GeV are distributed by a beam spreader, designed to deliver individual bunches from a CW linac to an array of independently configurable FEL beamlines with nominal bunch rates up to 100 kHz in each FEL, and with even pulse spacing. The final beamline in the spreader array will use DC components in place of pulsed kickers, and allow the full bunch rate from the linac to be delivered to the downstream FEL. This design study uses a pulsed magnetic kicker to initiate the deflection of a bunch. The schematic of the beam spreader is shown in Fig 1.

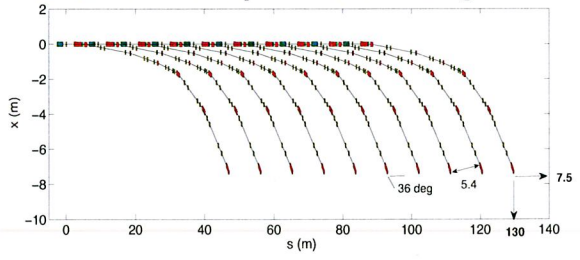

Figure 1: The schematic of a beam spreader scheme directing 1 MHz electron bunches from the Linac into 10 FEL lines.

The FEL beam lines are bent horizontally with a 36 degree angles to optimize beam distribution within a reasonable longitudinal footprint, and providing a 5.4 m separation between the undulators. Each beam line consists of a "take-off" section and a beam transport section made up of two triple-bend achromats providing

*Work supported by the Director, Office of Science, of the U.S. Department of Energy under Contract No. DE-AC02-05CH11231
#mplacidi@lbl.gov

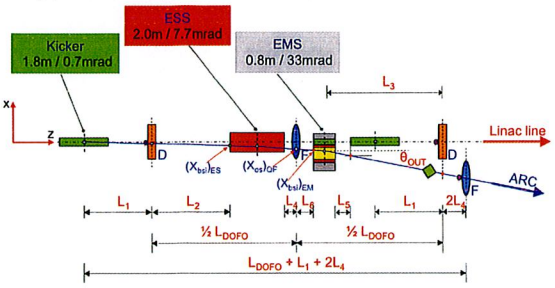

Figure 2: Schematic of a take-off section heading into a two-achromats branch line.

achromatic and isochronous beam transport properties for the beams at the entrance of the FELs. The spreader footprint in the shown configuration is 7.5x130 m^2.
Design requirements for the spreader are:

- Transport the electron beam from the end of the linac to any FEL line with minimal beam loss at any operational electron energy and rate.
- Allow one un-deflected diagnostic beam line in the straight-ahead direction.
- Include adequate vacuum chamber aperture to transport a low-energy beam.
- Include a fast, stable, reliable beam switching system (kickers) to direct any bunch into any FEL or diagnostic line within <1 μs at a kicker stability level which produces a peak horizontal position jitter in the undulator about 5% of the beam size there.
- Must not degrade the electron beam (time-sliced) brightness by more than about 10%.
- Include adjustable energy halo collimation systems to protect the undulators.
- Include MPS systems (toroid comparators and beam loss monitors) to switch off or rate-limit the electron beam quickly when large beam losses occur.
- Include adequate vacuum chamber cooling at high-power beam loss or beam-induced radiation locations (strong bends, small bellows, collimators, etc) where needed.
- Include charge, beam position, beam loss, relative bunch length, energy spread, and beam profile monitors as needed to setup the beam deflection.

In addition, the electron beam spreader should include one electron energy spectrometer per beam line, which can resolve relative energy changes as small as 10^{-6}.

The Take-off Section

The take-off section for one branch line is schematically shown in Fig. 2. Bunches directed to the two achromats beam transport arcs are deflected about 0.7

mrad by a 1.8 m long fast kicker at a repetition rate of up to100 kHz and by 7.7 mrad by a DC electrostatic septum (ESS) before reaching a DC electromagnetic septum (EMS) where they receive the final deflection into the Arcs. The focusing lattice is of the "DOFO" type with the first D-quad helping the kicker deflection. The Take-Off scheme can be designed for a cell length L_{DOFO} down to 9.2 m in order to provide a 5.4 m horizontal separation between the undulator lines with a 36 deg total deflection.

For sake of compactness the quadrupoles in the DOFO lattice are "J. Tanabe septum-type" slim quadrupoles, with a 245 mm mechanical width, a 60 mm bore diameter and a 0.20 m length [2]. The DOFO cell phase advance of 45 deg is chosen in order to use the same type of quadrupoles as in the preceeding beam diagnostics line. The required 7 T/m gradient fits comfortably within the quadrupole specifications.

Table 1: Main Parameter List for the Take-off Section

Parameter	Symbol	Unit	Value
Beam Energy	E	GeV	2.6
DOFO Cell length	L_{DOFO}	m	9.2
Cell Phase Advance	$\Delta\mu_{cell}$	deg	45
Quad Gradient	G	T/m	7.2
Quad Effective Length	L_Q	m	0.20
Quad bore diameter	d_Q	mm	60.0
Trajectory offset in QF	$(Xos)_{QF}$	mm	14.9
Kicker deflection	θ_k	mrad	0.7
Kicker length	L_k	m	1.8
ESS deflection	θ_{ESS}	mrad	7.7
ESS length	L_{ESS}	m	2.0
EMS deflection	θ_{EMS}	mrad	33.0
EMS length	L_{EMS}	m	0.8
Beams sep. at ESS entr.	$(Xbsi)_{ES}$	mm	3.1
Beams sep. at EMS entr.	$(Xbsi)_{EM}$	mm	18.0
ESS septum thickness	X_{ES}	mm	0.10
EMS septum thickness	X_{EM}	mm	5.25
Total Arc deflection	θ_{ARC}	deg	36

The Kicker

The requirements for the NGLS kickers are summarized in [3]. Both strip line and conventional ferrite loaded kicker magnets have been investigated, with a preference for the ferrite magnet because of high magnetic gain and better control of the beam impedance since a ceramic chamber is required. A system using several short ferrite magnets, each driven by a parallel array of MOSFET switches, is shown in Fig. 3. The maximum length of the magnets is limited by the maximum operating voltage of the MOSFETs (~700 V) and by the magnet fill time assumed to be less than 30 ns with the particular ferrite used (CMD500).

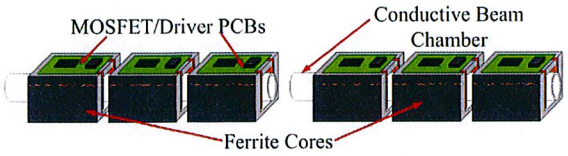

Figure 3: Layout of kicker system.

The Electrostatic Septum (ESS)

An electrostatic separator ESS is being considered to provide an additional deflection with the aim of relaxing the requirements from the fast-pulsed kicker for a better reliability and reproducibility. The two combined deflections provide a reasonable beam separation at the entrance of the electromagnetic septum (EMS) dipole without involving large offsets in the DOFO quadrupoles. The deflection from an electrostatic field E_{ESS} across the gap g_{ESS} between the electrodes is:

$$\tan\theta_{ESS} = \frac{L_{ESS}\,E_{ESS}}{\beta cp} \approx \frac{L_{ESS}}{E}\frac{V_{ESS}}{g_{ESS}}$$

A 10 MV/m field over a 2 m active length L_{ESS} would deflect a 2.6 GeV electron beam by 7.7 mrad. We envisage an operational figure of 70 kV for the applied high voltage V_{ESS} in order to limit the conditioning high voltage to about 100kV. This requires the septum to be built with a horizontal gap g_{ESS} =7.0 mm. A straight septum geometry (Fig. 4) complying with the beam excursion X_b=9.3 mm plus beam clearance to the electrodes would require a horizontal gap g_{ESS} ~14 mm, exceeding the above requirements. An alternative solution consists in adopting electrodes bent along the beam trajectory following experience gained at CERN [4] on the construction of ES separators of similar length. A properly kinked 7 mm gap could provide a reasonable aperture to the deflected beam and the desired E_{ESS} deflecting field. This geometry would also contribute in reducing the impedance to the un-deflected beam, whose distance from the thin electrode increases along the path.

These advantages are potentially compromised by problems connected with the exposure of the second thin electrode to synchrotron radiation from the deflected electron bunches in the initial portion of their trajectory. Radiation from the 2.6 GeV electrons entering the ESS under a 0.8 mrad incoming angle (Fig. 4) is emitted in a cone of $1/\gamma$~200 μrad aperture and is intercepted by the kinked electrode unless the gap aperture is large enough to avoid the interference. Consequences from foil local heating and electron photo-emission require further investigation.

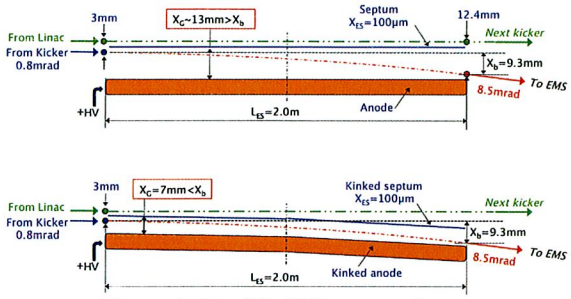

Figure 4: Possible ESS geometries.

The Electromagnetic Septum (EMS)

The EMS is an electromagnet "window-frame-type" modified in order to provide a "zero-field" channel for the transmission of the un-deflected beam (Fig. 5).

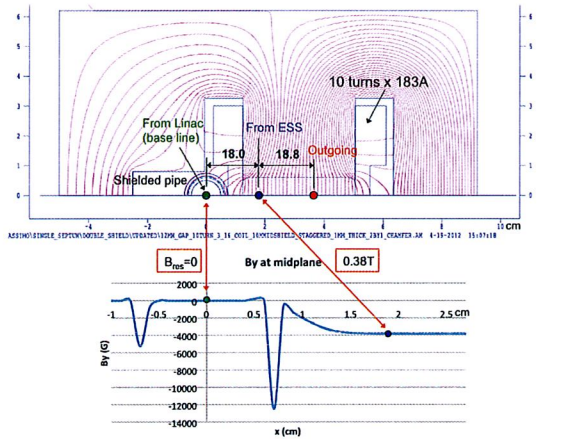

Figure 5: Vertical cross section of the EMS dipole showing the positions of the base line beam and the deflected one both at the incoming and the outgoing coordinates.

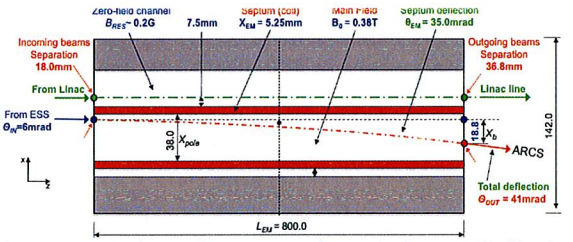

Figure 6: Horizontal cross section of the EMS dipole showing the excursion of the deflected beam inside the 38-mm wide gap and the field-free channel transmitting the un-deflected beam.

Its "staggered" coils use a small conductor size in the 6-turns inner layer and the 4-turns external one. The septum thickness at median plane is that of the single layer, about 5 mm, which fits the 18 mm separation of the incoming beams. The magnet design provides a 0.38 T magnetic field in the 12 mm main gap for up to a 35 mrad deflection at E=2.6 GeV. A horizontal cross section of the EMS is shown in Fig. 6. Additional tips at the polepiece profile provide full compensation of the field gradient across the ~20 mm extension of the beam excursion. A shielded pipe in the "zero-field" channel compensates the residual field down to 0.2 G. The EMS excitation current is 183 A for a maximum DC power of 3.2 kW.

The Branch Beam Transport Line

The beam transport line from the Linac to FEL line needs to be carefully designed to meet the spreader requirements mentioned above. Importantly, it must be achromatic to avoid the emittance exchange between the longitudinal and the transverse phase spaces, and to avoid transverse beam jitter due to an energy jitter. The transport line must also be isochronous to avoid lengthening of the bunch, and to avoid the time-of-flight jitter due to the energy jitter. The Twiss functions of a typical branch beam line are shown in Fig. 7.

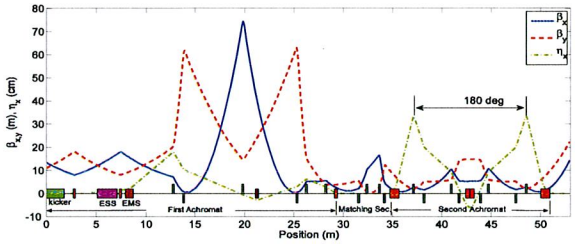

Figure 7: Twiss functions of one typical branch beam line.

Each line has two distinct "triple-bend" achromats designed to be isochronous and connected by a dispersion-free qaudrupole matching section. In the first achromat, the kicker, the septa and the off-set in the QD and QF quadrupoles are functionally equivalent to one bending magnet. An additional pair of bending magnets completes the orbit bending of 5.67 degrees.

The second achromat has a mirror-symmetric structure, and three identical bends provide a total orbit bending of 30.33 degrees. The total bending angle of the beam line is 36 degrees, separating each FEL line by 5.4 m.

REFERENCES

[1] J. Corlett et al., "Next Generation Light Source R&D and Design Studies at LBNL", *These proceedings.*

[2] J. Tanabe, "Recirculating Linac Septum Quadrupole Designs", Tech. Note October 22, 2001.

[3] M. Placidi, "Update on Kicker Development for the NGLS", *These proceedings.*

[4] M. Barnes et al., "Injection and Extraction: Septa", proc. CAS 2009 'Specialised course on Magnets', Bruges.

This document was prepared as an account of work sponsored by the United States Government. While this document is believed to contain correct information, neither the United States Government nor any agency thereof, nor The Regents of the University of California, nor any of their employees, makes any warranty, express or implied, or assumes any legal responsibility for the accuracy, completeness, or usefulness of any information, apparatus, product, or process disclosed, or represents that its use would not infringe privately owned rights. Reference herein to any specific commercial product, process, or service by its trade name, trademark, manufacturer, or otherwise, does not necessarily constitute or imply its endorsement, recommendation, or favoring by the United States Government or any agency thereof, or The Regents of the University of California. The views and opinions of authors expressed herein do not necessarily state or reflect those of the United States Government or any agency thereof or The Regents of the University of California.

This work was supported by the Director, Office of Science, Office of Fusion Energy Sciences, of the U.S. Department of Energy under Contract No. DE-AC02-05CH11231.